R. & M. No. 2999
(17,428)
A.R.C. Technical Report

MINISTRY OF SUPPLY

AERONAUTICAL RESEARCH COUNCIL
REPORTS AND MEMORANDA

# R.A.E. High-Speed Wind-Tunnel Tests of the Trailing-edge Controls on a Delta Wing with 52-deg Sweepback

*By*
K. W. NEWBY, D.AE.



LONDON: HER MAJESTY'S STATIONERY OFFICE
1957
PRICE 6*s.* 6*d.* NET

# R.A.E. High-Speed Wind-Tunnel Tests of the Trailing-edge Controls on a Delta Wing with 52-deg Sweepback

*By*

K. W. NEWBY, D.Ae.

COMMUNICATED BY THE PRINCIPAL DIRECTOR OF SCIENTIFIC RESEARCH (AIR), MINISTRY OF SUPPLY

*Reports and Memoranda No.* 2999*

*January*, 1952

*Summary.*—Tests have been made in the Royal Aircraft Establishment 10-ft × 7-ft High-Speed Wind Tunnel to determine the effectiveness of trailing-edge controls on a delta wing, of 52 deg leading-edge sweep and NACA 0010 section (trailing-edge angle 12 deg) using the half-model technique. Three plain controls were tested—an inboard control, an outboard control, and the two combined.

For a trimmed $C_L$ of 0·2 to 0·3, there is no appreciable reduction of effectiveness on any control below $M = 0·87$. For $M = 0·94$, all controls have at least 50 per cent. of their low-speed effectiveness in pitch and roll. At higher incidence, reductions in effectiveness occur, particularly near $M = 0·87$, but are mostly associated with the effects of control deflection on tip stalling. The tests were made at $R = 1·8 \times 10^6$ (based on mean chord) and hence the results may give a pessimistic idea of the behaviour at high Reynolds number. The pitching-moment characteristics show that cropping the pointed wing tip alleviates the tip stalling, as expected. For the cropped wing, the backward shift, with Mach number, of the aerodynamic centre at $C_L = 0·2$ is less than $0·04\bar{c}$ up to $M = 0·93$

1. *Introduction.*—Various tests have shown that severe reductions or even reversal of the effectiveness of trailing-edge controls may occur at high subsonic speeds. Such effects are more serious on wings having either large trailing-edge angles or little trailing-edge sweep. In particular, it was expected that this might prove an objection to the use of wings of a delta plan-form.

The tests described in this report were made on a delta wing having 52-deg sweep at the leading edge and an NACA 0010 aerofoil section with a trailing-edge angle of 12 deg. Three plain controls were tested: an inboard (elevator) control, an outboard (aileron) control and the two controls combined (elevon).

Overall measurements, with various combinations of control setting were made with a wing of a true delta plan-form (*i.e.*, with a pointed tip). The pointed tip was then removed, giving the wing a taper ratio of 0·115 to avoid the effects of an early stall at the tips: and the measurements with the controls undeflected were repeated.

Pressure plotting measurements were made at four spanwise stations. The analysis of these data is to be reported separately; the information has however been used in this report to interpret the overall measurements. The tests were made by the half model technique before a satisfactory seal had been developed to prevent air flowing into the working section through the gap between the wing stub and the tunnel floor. The overall measurements include the forces on a body which was made integral with the wing and which was mostly submerged within the boundary layer on the tunnel floor. For these reasons, no drag results are included in this report. However, since the inboard end of the elevator is well outside the tunnel boundary layer, there is no reason to believe the measurements of control effectiveness were affected.

* R.A.E. Report Aero. 2451, received 14th June, 1952.

2. *Experimental Details.*—2.1. *Details of Model.*—The model was constructed of laminated teak, except for the controls which were of plywood, held in position by steel plates inset on the wing chord line. The surface finish applied was ' Pheenoglaze Polish '.

The basic triangular wing plan-form (Fig. 1) was of 30-in. semi-span, with 52-deg sweepback on the leading edge, the tip being rounded off to a model semi-span of 29·7 in. (Aspect ratio = 3·02.) The outboard 3·15 in. of the wing was made detachable to leave a wing having a taper ratio of 0·115 and an aspect ratio of 2·44. There was no twist or dihedral on the wing, the aerofoil being of NACA 0010 section with 1·1 per cent chord leading-edge radius and 12-deg trailing-edge angle throughout the span. A slender body having a 5-deg droop on the nose was fixed to the root section of the wing.

The elevator control extended from 25·2 per cent to 53·2 per cent and the aileron from 53·2 per cent to 89·4 per cent of the semi-span, the hinge lines of both controls being slightly swept-back, and situated at 15 per cent of the local chord from the trailing edge. The angular settings tested for both controls were 0, −3, −5, −7, −10 and −20 deg measured in a plane perpendicular to the wing trailing edge.

Twenty-two wing surface static-pressure tubes were provided at each of four spanwise stations (Fig. 1), the ends of the tubes remote from the wing surface being sealed during the force tests.

Further details of the model are summarised in Table 1.

The wing stub of the model was mounted through angle plates (Fig. 1) on the six-component mechanical balance. A small gap was left between the wing stub and the tunnel floor turntable so that the forces on the wing were transmitted to the balance. There was no seal to prevent air flowing through this gap.

2.2. *Details of Tests.*—The following model configurations were tested over the Mach number range $M = 0{\cdot}5$ to $M = 0{\cdot}94$.

| | $\eta$ (*deg*) | $\xi$ (*deg*) | $R \times 10^{-6}$ | *Incidence range* $\alpha$ (*deg*) | *Aspect ratio* $A$ | Tip shape |
|---|---|---|---|---|---|---|
| Controls undeflected | 0 | 0 | 1·8 | −1 to 12 | 3·02 | ' Pointed ' tip |
| | 0 | 0 | 1·0 | −1 to 12 | 3·02 | ,, ,, |
| | 0 | 0 | 2·0 | −1 to 12 | 2·44 | ' Squared ' tip |
| Controls deflected separately | − 3 | 0 | 1·8 | −1 to 8 | 3·02 | ' Pointed ' tip |
| | − 7 | 0 | 1·8 | −1 to 8 | 3·02 | ,, ,, |
| | −10 | 0 | 1·8 | −1 to 8 | 3·02 | ,, ,, |
| | 0 | − 3 | 1·8 | −1 to 8 | 3·02 | ,, ,, |
| | 0 | − 5 | 1·8 | −1 to 8 | 3·02 | ,, ,, |
| | 0 | − 7 | 1·8 | −1 to 8 | 3·02 | ,, ,, |
| | 0 | −10 | 1·8 | −1 to 8 | 3·02 | ,, ,, |
| | −10 | 0 | 1·0 | −1 to 8 | 3·02 | ,, ,, |
| | −20 | 0 | 1·0 | −1 to 8 | 3·02 | ,, ,, |
| | 0 | −10 | 1·0 | −1 to 8 | 3·02 | ,, ,, |
| | 0 | −20 | 1·0 | −1 to 8 | 3·02 | ,, ,, |
| Controls deflected together | − 5 | − 5 | 1·8 | −1 to 8 | 3·02 | ,, ,, |
| | −10 | −10 | 1·8 | −1 to 8 | 3·02 | ,, ,, |

*Note:*

$\eta$ Inboard control setting (elevator angle)

$\xi$ Outboard control setting (aileron edge)
(The controls deflected together gave the effect of an elevon.)

$R$ Reynolds number based on standard mean chord.

The positioning of the model on the mechanical balance was such that pitching moments were measured about the 0·54 centre-line–chord point.

For all configurations lift, pitching moment and rolling moment were measured.

After the main tests had been completed, silk tufts, attached to the upper surface of the wing by means of cellophane self-adhesive tape, were photographed at various Mach numbers and incidences with the controls neutral.

2.3. *Corrections Applied to the Results.*—The Mach number at the model station was corrected for blockage according to the method of Ref. 1, account being taken of the blockage effect on the pressure measured at the wind-speed reference hole at the upstream end of the working-section. Typical values for this blockage correction at the model are given below.

| | | | | | | | |
|---|---|---|---|---|---|---|---|
| $\alpha = 0$ deg | | | | | | | |
| $M$ corrected .. | 0·500 | 0·700 | 0·800 | 0·850 | 0·900 | 0·920 | 0·940 |
| $\Delta M$ .. .. | 0 | 0·001 | 0·003 | 0·006 | 0·012 | 0·018 | 0·029 |
| $\alpha = 8$ deg | | | | | | | |
| $M$ corrected .. | 0·500 | 0·700 | 0·800 | 0·850 | 0·900 | 0·920 | 0·940 |
| $\Delta M$ .. .. | 0 | 0·001 | 0·003 | 0·006 | 0·016 | 0·024 | 0·036 |

The incidence of the model was corrected to allow for the sidewash of the airflow in the tunnel, the geometric incidence being decreased by 0·45 deg throughout the speed range. The available data were not sufficiently precise to justify assuming any variation of this correction with Mach number.

Tunnel constraint corrections on the lifting surface have not been applied, but this should not affect the comparison of the results for different control settings.

3. *Discussion of Results.—Note.*—Pitching moments were measured about the 0·54 centre-line–chord point.

3.1. *Model with Pointed Tip and Controls Neutral.*—For all Mach numbers below about 0·9, the lift curves are sensibly linear up to a lift coefficient $C_L = 0{\cdot}3$ (Fig. 2). For $R = 1{\cdot}8 \times 10^6$, $M = 0{\cdot}5$, the-lift curve slope $(\partial C_L/\partial\alpha)_M$ is 3·04 which is in good agreement with an estimated value of 3·0. $(\partial C_L/\partial\alpha)_M$ increases slowly with Mach number up to $M = 0{\cdot}9$ but less rapidly than would be predicted by linear perturbation theory (Fig. 3a). For $R = 1 \times 10^6$, in this Mach number range, $(\partial C_L/\partial\alpha)_M$ is lower by about 2 per cent.

The variation of the pitching moment $C_m$ with $C_L$ is shown in Fig. 4. The effect of Mach number on the pitching moment at zero lift $C_{m0}$ is small (Fig. 5a), the measured values varying from $-0{\cdot}016$ at $M = 0{\cdot}5$ to $-0{\cdot}006$ at $M - 0{\cdot}94$. These actual values are almost certainly influenced by the effects of the tunnel boundary layer, but the nose-down droop of the forward part of the body and the accompanying difference in shape between the upper and lower wing-body junctions may be sufficient to account for the measured results—at least, at low speed.

The aerodynamic centre at zero lift (Fig. 5b) at low speed is $0{\cdot}05\bar{c}$ behind the 0·54 centre-line–chord point or $1{\cdot}13\bar{c}$ behind the leading-edge apex, compared with an estimated value of $1{\cdot}16\bar{c}$. With increasing Mach number up to $M = 0{\cdot}87$ and at $R = 1{\cdot}8 \times 10^6$, it moves steadily back by about the amount predicted by linear theory. For $R = 1 \times 10^6$, this backward movement does not occur, presumably owing to boundary-layer effects, particularly over the tip sections.

The behaviour of silk surface tufts showed that as the incidence is increased for a given Mach number, circulatory flow, associated with a vortex shed from the leading edge, appears near the tip. The vortex core moves inwards with increases in either incidence or Mach number; outboard

of this core, the flow is disturbed. These effects have been found in various flow surveys on swept and delta wings, and the tufts probably give a reasonable qualitative picture even though some of the flow disturbance may not be present when the tufts are not there.

The areas of the wing apparently affected by tip stalling at $R = 1{\cdot}8 \times 10^6$ are shown in Fig. 3c; for $M = 0{\cdot}5$, stalling starts at the tip at an incidence of about 4 deg ($C_L \doteq 0{\cdot}2$), while above $M = 0{\cdot}7$, it has begun at 2 deg. Because of the wing geometry, tip stalling has more influence on the pitching-moment characteristics than on $(\partial C_L/\partial\alpha)_M$: *e.g.*, at low speed, the loss in lift over the outboard part of the wing results in the model becoming progressively less stable between $C_L = 0{\cdot}2$ and $0{\cdot}4$, neutral stability about $0{\cdot}54$ centre-line–chord occurring near $C_L = 0{\cdot}4$ ($R = 1{\cdot}8 \times 10^6$), while $(\partial C_L/\partial\alpha)_M$ decreases slightly above $C_L = 0{\cdot}3$. Above $C_L = 0{\cdot}5$, the longitudinal stability increases again: it is probable that, then, the flow over the tip sections has completely separated and there is little pressure recovery over the rear of the sections. This would result in a backward movement of the local centres of pressure (this was shown by the pressure-plotting data on this wing).

The spread of tip stalling with increasing Mach number (Fig. 3c) results in

(i) the changes in $(-\partial C_m/\partial C_L)_M$ with $C_L$ occurring at lower values of $C_L$ as the Mach number is increased (Fig. 4)

(ii) there being practically no change in $(-\partial C_m/\partial C_L)_M$ with $M$ below $M = 0{\cdot}87$ for $C_L = 0{\cdot}2$ since the growth of the destabilizing effect of the tip stall roughly balances the increase in stability due to compressibility effects, which was found at $C_L = 0$ (Fig. 5b).

The tip stalling effects noted above are probably subject to serious scale effect. This is illustrated by a comparison of the $C_m$ vs. $C_L$ curves at $R = 1 \times 10^6$ and $1{\cdot}8 \times 10^6$, based on mean chord (Fig. 6). For example, for $R = 1 \times 10^6$, $M = 0{\cdot}5$, the model becomes unstable above about $C_L = 0{\cdot}3$. The Reynolds number is smaller near the tip and at full scale, the tip stalling effects should be postponed to higher incidences.

Above $M = 0{\cdot}90$, certain other effects may be noted:

(*a*) at small incidences, $(\partial C_L/\partial\alpha)_M$ decreases with $M$ and this is accompanied by a forward movement of the aerodynamic centre. The pressure-plotting data, to be reported later, showed that under these conditions, the shock wave off the upper surface is further forward than the one on the lower surface except near the root. Hence the positive lift over the forward part of the chord is partly balanced by some negative lift towards the rear. This condition occurs only at small incidences; as the incidence is increased, the supersonic region on the lower surface contracts and the breakaway behind the upper surface shock becomes more pronounced, thus increasing the suctions over the rear upper surface.

(*b*) at high values of $C_L$, there is a rapid increase in $(-\partial C_m/\partial C_L)_M$, e.g., for $C_L = 0{\cdot}4$, $(-\partial C_m/\partial C_L)_M$ is $0{\cdot}15$ higher for $M = 0{\cdot}95$ than at low speed. Fig. 5c shows that this effect is greatly reduced in this Mach number range by the removal of the pointed tip and hence that it is a function of the peaky spanwise lift distribution on the true delta.

3.2. *Effect of Removing the Pointed Tip.*—The pointed tip was removed with the object of delaying the onset of the tip stall to a higher incidence: increasing the taper ratio of a wing modifies the spanwise lift distribution in such a way that the local values of $C_l$ near the tip are reduced for a given overall $C_L$.

A comparison of the $C_m$ vs. $C_L$ curves in Fig. 4 shows that the performance was improved; for the wing without the pointed tip, the pitching-moment curves for Mach numbers below $0{\cdot}9$ are sensibly linear up to $C_L = 0{\cdot}5$. (The stability is rather less at small incidences but other tests have shown that this effect can be eliminated by inducing forward transition. Hence the effect is associated with a movement of transition position with incidence and may be peculiar to the flow at low Reynolds numbers.)

The considerable improvement in the pitching-moment characteristics is further illustrated by comparing Figs. 5b and 5c. The position of the aerodynamic centre moves slowly back with increasing Mach number but the shift does not amount to more than about $0{\cdot}03\bar{c}$ in the test Mach number range from $0{\cdot}5$ to $0{\cdot}93$. The variation with Mach number is in very good agreement with that predicted by theory. Another improvement is that mentioned at the end of section 3.1, *i.e.*, the postponement to higher Mach numbers of the large increase in stability at high values of $C_L$.

In addition to altering the taper ratio, the removal of the tip also reduced the wing aspect ratio. This accounts for the lower value of $(\partial C_L/\partial\alpha)_M$ at low speed (Fig. 3b). However, the increase of $(\partial C_L/\partial\alpha)_M$ with $M$ up to $M = 0{\cdot}9$ is more rapid than before and is now in agreement with theoretical prediction—an interesting comparison with the results for the wing with pointed tip. As a result, near $M = 0{\cdot}9$, both wings, despite their differing aspect ratios, have about the same value of $(\partial C_L/\partial\alpha)_M$.

3.3. *Elevator Control Effectiveness.*—$C_m$ vs. $C_L$ curves for $M = 0{\cdot}5$, $0{\cdot}87$, $0{\cdot}90$, $0{\cdot}93$ are shown in Fig. 6 for the different elevator angles tested. In Figs. 9, 10, $C_L$ and $C_m$ are given as functions of incidence and elevator deflection by means of a carpet presentation. The variation of the lift and pitching-moment effectiveness with Mach number for an incidence corresponding to a typical cruising $C_L$ of $0{\cdot}2$ is plotted in Figs. 17 and 18 and elevator angles to trim in Fig. 20.

3.3.1. *Variation with Mach number of elevator effectiveness under typical cruising conditions.*—From the variation of $\Delta C_L$ and $\Delta C_m$ with $M$ for different values of $\eta$ at an incidence corresponding to $C_L = 0{\cdot}2$ with controls neutral, as plotted in Figs. 17 and 18, it can be seen that no appreciable reduction of elevator effectiveness occurs below $M = 0{\cdot}90$. Below $M = 0{\cdot}90$, there is a small decrease of lift effectiveness and a slight increase of pitching effectiveness with Mach number. Reference to the pressure-plotting data has shown that the latter is associated with the growth of a supersonic region followed by a breakaway on the lower surface of the control.

Above $M = 0{\cdot}90$, the elevator effectiveness decreases with Mach number but even at $M = 0{\cdot}94$, the lift effectiveness is still about 70 per cent of its low-speed value and the pitching effectiveness is probably better than this. The reduction of effectiveness is almost entirely caused by the growth of a supersonic region of flow ahead of the elevator.

3.3.2. *Elevator effectiveness at higher incidences.*—The most marked feature of the results is the reduction in pitching effectiveness which occurs at incidences between $\alpha = 4$ deg and 6 deg. The effect is present to a slight extent at low speeds but becomes more pronounced between $M = 0{\cdot}8$ and $0{\cdot}9$ (*e.g.*, the curves $\eta = -7$ deg and $-10$ deg in Fig. 10a for $M = 0{\cdot}83$ and $0{\cdot}87$). The most likely explanation of these effects is that up-deflection of the elevator alleviates the stall over the wing just outboard of the elevator. This theory is supported by the tuft results of Fig. 3c which show that with the controls set neutral, the tip stall has spread to about the outboard end of the elevator at the incidence corresponding to the loss of pitching effectiveness. Presumably the boundary layer over the inboard upper surface is diverted by the deflection of the elevator and so is relatively thin just outboard of the elevator. The suggestion that the inboard spread of the tip stall is retarded or postponed to a higher $C_L$ by the action of the elevator can be appreciated best by reference to the shape of the $C_m$ vs. $C_L$ curves in Fig. 6. Other points in favour of the suggestion are: first, the fact that by comparison, the lift effectiveness is only influenced slightly (Fig. 9) and secondly, the behaviour at $R = 1 \times 10^6$ (Fig. 10b). At the lower Reynolds number, the reduction in pitching effectiveness for $\eta < 10$ deg occurs at smaller values of $\alpha$ than for $R = 1{\cdot}8 \times 10^6$ while for incidences between 4 deg and 6 deg, a larger control deflection (between 10 deg and 20 deg) is needed to produce the effect (Fig. 10b). These characteristics can be explained in terms of the more serious tip stall at the lower Reynolds number. The evidence in support of the explanation is not conclusive but considered in full, seems reasonable. If the explanation is correct, then at flight Reynolds numbers, the loss of pitching effectiveness would be delayed to a much higher incidence.

For Mach numbers above 0·90, the effect is not so serious. The pressure-plotting data suggest that this is because, after a strong shock wave has developed on the upper surface, the influence of the up-deflected elevator on the position of this shock is dominant.

3.3.3. *Elevator effectiveness at large deflections.*—Fig. 9b shows that the lift effectiveness decreases for values of $\eta$ approaching — 20 deg at both low and high incidences (for intermediate incidences, such as 4 deg, it remains fairly constant). The effect is already present at low speeds and becomes more marked with increasing Mach number.

The effect at high incidence is probably genuine but at low incidence it occurs partly because the lift effectiveness at low Reynolds number and small deflections is increased by a separation behind the hinge line of the control on the lower surface. At higher Reynolds numbers, this would be expected to occur only for larger control deflections and so the resulting variation of $C_L$ with $\eta$ would be more linear than is shown in Fig. 9b.

3.3.4. *Elevator angle to trim.*—The values of elevator angle to trim are given in Fig. 20 and call for little comment. The displacement of the curves for $C_L < 0{\cdot}2$, being caused by the measured variation of $C_{m0}$ with $M$ referred to in section 3.1 may not be genuine. The variations for $C_L > 0{\cdot}2$ arise from the various effects discussed above and so the quantitative variation of $\eta_{\text{trim}}$ with $M$ may be less at flight Reynolds numbers. However, the increase in up-elevator required for trim above $C_L = 0{\cdot}3$ as the Mach number is increased above 0·9 should still apply, at least qualitatively.

3.4. *Aileron Control Effectiveness.*—$C_m$ vs. $C_L$ curves, for the different aileron settings tested, are given in Fig. 7, while $C_L$, $C_m$ and $C_l$ are given in Figs 11 to 13 as functions of incidence and Mach number. The variations of the lift, pitching and rolling effectiveness of the aileron with Mach number are plotted in Figs. 17 to 19 for an incidence corresponding to a typical cruising $C_L$ of 0·2.

These results are probably even more subject to scale effect than those for the elevator discussed above. Even at moderate incidences, the aileron effectiveness is altered by the influence of the control deflection on the tip stall and at moderate deflections, by a breakaway of flow over the control lower surface. The reductions in control effectiveness that are caused by these effects would not be present to the same extent at higher Reynolds numbers.

3.4.1. *Variation with Mach number of aileron effectiveness under typical cruising conditions.*—The variation of effectiveness with Mach number is shown in Figs. 17 to 19 for an incidence corresponding to $C_L = 0{\cdot}2$ when the controls are neutral.

For small aileron deflections, *e.g.*, — 5 deg, there is little variation with Mach number up to $M = 0{\cdot}94$ for lift or pitch ; the effectiveness in roll decreases at $M = 0{\cdot}92$.

For larger up-deflections, the reductions in effectiveness with increasing Mach number appear to be more pronounced. Even from $M = 0{\cdot}5$ to 0·87, there is a gradual reduction of lift and rolling effectiveness while the effectiveness in pitch remains about the same, instead of increasing with Mach number, as for the elevator. The pressure-plotting results suggest that these characteristics may be caused partly by a breakaway of the flow over the lower surface of the control, and partly by the fact that even at this incidence the change in spanwise loading due to deflecting the control is sufficient to reduce the tip stalling tendency (Fig. 3c).

Above $M = 0{\cdot}87$, the effectiveness for large deflections decreases more rapidly. At $M = 0{\cdot}94$, for example, increasing the deflection from, say, — 7 deg to — 10 deg has little effect on either $C_L$ or $C_l$ and for — 10 deg, the effectiveness in roll is only about 50 per cent of its value at low speed. The effectiveness in pitch decreases less seriously. The reasons for these effects at high Mach number will be discussed in detail in the later report on the pressure-plotting data. It will then be seen that the effectiveness at high Mach numbers may be different for positive and

negative deflections and so values of the effectiveness in roll deduced merely from the results for up-deflection (as here) may be misleading quantitatively. Also it appears that the reductions in effectiveness may be still present at high Reynolds numbers.

3.4.2. *Aileron effectiveness at higher incidences.*—There is a marked reduction of the aileron effectiveness in pitch (Fig. 12) as the incidence is increased; *e.g.*, for $M = 0{\cdot}87$ and $\alpha = 8$ deg, altering from $-10$ deg to $-20$ deg gives no further change in $C_m$. The effectiveness in roll is also reduced, particularly for large deflections but the lift effectiveness varies only slightly (Figs. 11, 13). These characteristics are consistent with the suggestion that up-deflection of the aileron tends to alleviate the tip stalling of the wing. (It was noted in section 3.1 that tip stalling principally effects $C_m$.) At the lower Reynolds number ($1 \times 10^6$), a larger deflection of the aileron is needed to produce a similar effect owing to the more severe tip stall. At high Reynolds numbers, the tip stall would be delayed to higher incidences and so the reductions in aileron effectiveness would be similarly postponed.

3.4.3. *Aileron effectiveness for large deflections.*—Figs. 11 to 13 show the variation of aileron effectiveness with Mach number and incidence. Losses in effectiveness occur

(i) at high incidence, particularly in pitch

(ii) at low incidence, in all components and especially in roll.

These effects may be exaggerated by a deflection of the model control under load but basically are probably caused by

(*a*) a breakaway of the flow over the control lower surface

(*b*) at high incidence, by the alleviation of the tip stall.

3.5. *Effectiveness of Combined Control (Elevon).*—$C_m$ vs. $C_L$ curves for the different elevon angles tested are given in Fig. 8 and $C_L$, $C_m$, $C_l$ carpets are presented in Figs. 14 to 16. The variations of the lift, pitching and rolling effectiveness with Mach number are plotted in Figs. 17 to 19 and the elevon angles to trim are given in Fig. 20.

In general, the results are similar to the sum of those obtained when the elevator and aileron are deflected separately.

The main features of the results are:

(i) in pitch, for deflections of about 5 deg, the elevon has about twice the effectiveness of the elevator (elevon area $= 1{\cdot}67 \times$ elevator area). For larger deflections the elevon effectiveness is reduced (*e.g.*, the aileron)

(ii) in roll, the elevon has about twice the effectiveness of the aileron (elevon area $= 2{\cdot}5 \times$ aileron area; elevon rolling arm to centre of area $= 0{\cdot}74 \times$ aileron rolling arm)

(iii) for small elevon deflections, *e.g.*, $-5$ deg, the effectiveness in pitch increases gradually with Mach number up to $M = 0{\cdot}9$ while the effectiveness in lift and roll remain sensibly unchanged. At higher Mach numbers, the effectiveness in all components decreases, but even for $M = 0{\cdot}94$, is over 70 per cent of the value at low speed.

(iv) with larger deflections (*e.g.*, $-10$ deg), the lift and rolling effectiveness decreases gradually with Mach number between $M = 0{\cdot}5$ and $0{\cdot}87$; above $M = 0{\cdot}87$, the reduction becomes more rapid. At $M = 0{\cdot}94$, the effectiveness in roll is about 60 per cent of the value at low speed.

4. *Conclusions.*—For a typical cruising $C_L$, say $0{\cdot}2$, the trailing-edge controls tested maintain their full effectiveness at least up to $M = 0{\cdot}87$ ($0{\cdot}90$ for the inboard elevator) and even at $M = 0{\cdot}94$ have at least 50 per cent of their low-speed effectiveness in both pitch and roll. The reductions in effectiveness will probably still be present at higher Reynolds numbers. The loss in elevator effectiveness at high speeds is largely a result of the growth of a local supersonic region over the wing upper surface.

At $\alpha = 5$ deg ($C_L \simeq 0{\cdot}3$), there is a rather marked loss of pitching effectiveness, particularly near $M = 0{\cdot}87$, with the inboard control deflected more than about 5 deg at $R = 1{\cdot}8 \times 10^6$. Also, at higher incidences and high speeds, the deflection of the aileron or elevon beyond a certain setting gives little further effect. Both these characteristics occur because the deflection of the control alleviates the tip stall. At higher Reynolds numbers, they would be delayed to higher incidences.

The reduction in longitudinal stability for the model with pointed tip at $R = 1{\cdot}8 \times 10^6$ occurs near $C_L = 0{\cdot}25$ at $M = 0{\cdot}87$ compared with a $C_L$ of $0{\cdot}35$ at $M = 0{\cdot}5$. Increase in Reynolds number should postpone this effect.

The improvement in the $C_m$ vs. $C_L$ curves resulting from the cropping of the wing tip to a taper of $0{\cdot}115$ suggests that the tip stalling was considerably reduced by this change.

For the wing with the square tip, $(-\partial C_m/\partial C_L)_M$ at $C_L = 0{\cdot}2$ increases by less than $0{\cdot}04$ between $M = 0{\cdot}5$ and $0{\cdot}93$.

---

## LIST OF SYMBOLS

| | |
|---|---|
| $\alpha$ | Model incidence |
| $\eta$ | Elevator deflection (positive, trailing edge down) |
| $\xi$ | Aileron deflection (positive, trailing edge down) |
| $\eta_E$ | Elevon deflection (positive, trailing edge down) |
| $C_L$ | Lift coefficient ($= L/\frac{1}{2}\rho V^2 S$) |
| $C_m$ | Pitching-moment coefficient about the $0{\cdot}54$ centre-line chord point ($=$ P.M.$/\frac{1}{2}\rho V^2 S\bar{c}$) |
| $C_l$ | Rolling-moment coefficient about the chord in the plane of symmetry of the aircraft ($=$ R.M.$/\frac{1}{2}\rho V^2(2S)(2b)$) |
| $L$ | Model lift |
| P.M. | Model pitching moment |
| R.M. | Model rolling moment due to controls |
| $S$ | Half-wing gross area |
| $\bar{c}$ | Standard mean chord |
| $b$ | Half-wing span |
| $A$ | Aspect ratio ($= 2b^2/S$) |
| $\frac{1}{2}\rho V^2$ | Dynamic head of free stream |
| $M$ | Mach number |

---

## REFERENCE


| *No.* | *Author* | *Title, etc.* |
|---|---|---|
| 1 | J. Y. G. Evans .. .. | Corrections to velocity for wall constraint in any 10-ft × 7-ft rectangular subsonic tunnel. R. & M. 2662. April, 1949. |

# TABLE 1

## *Model Data*

*Wing (pointed tip)*

| | |
|---|---|
| Area of half model | 4·062 sq ft |
| Span of half model | 2·475 ft |
| Standard mean chord | 1·641 ft |
| Tip chord | 0 |
| Centre-line chord | 3·250 ft |
| Taper ratio (tip chord/root chord) | 0 |
| Aspect ratio | 3·02 |
| Aerofoil section | Symmetrical NACA 0010 |
| Sweepback of leading edge | 52 deg 26 min |
| Sweepback of trailing edge | 0 deg |
| Dihedral | 0 deg |
| Geometric twist | 0 deg |
| Wing-body angle (nose of body) | 5 deg |

*Wing (pointed tip removed)*

| | |
|---|---|
| Area of half model | 4·009 sq ft |
| Span of half model | 2·212 ft |
| Standard mean chord | 1·812 ft |
| Tip chord | 0·374 ft |
| Centre-line chord | 3·250 ft |
| Taper ratio | 0·115 |
| Aspect ratio | 2·44 |

*Moment reference point* (All pitching moments measured about this point)

| | |
|---|---|
| Distance below chord line | 0 ft. |
| Distance behind leading edge of centre-line chord | 1·756 ft |
| Per cent centre-line chord aft of leading-edge apex | 54 per cent |
| Distance behind mean quarter-chord point: | |
| Wing with pointed tip | 0·131 ft (0·080$\bar{c}$) |
| Wing with pointed tip removed | 0·149 ft (0·082$\bar{c}$) |
| Distance of mean quarter-chord point aft of leading-edge apex: | |
| Wing with pointed tip | 1·625 ft |
| Wing with pointed tip removed | 1·607 ft |

*Elevator control*

| | |
|---|---|
| Span per side | 0·675 ft |
| Area aft of hinge line per side | 0·206 sq ft |
| Inboard end of elevator from wing centre-line | 0·600 ft |
| Hinge line 15 per cent chord from trailing edge | |

*Aileron control*

| | |
|---|---|
| Span per side | 0·938 ft |
| Area aft of hinge line per side | 0·138 sq ft |
| Inboard end of aileron from wing centre-line | 1·275 ft |
| Hinge line 15 per cent chord from trailing edge | |

*Elevon control*

| | |
|---|---|
| Span per side | 1·613 ft |
| Area aft of hinge line per side | 0·344 sq ft |
| Inboard end of elevon from wing centre-line | 0·600 ft |
| Hinge line 15 per cent chord from trailing edge | |

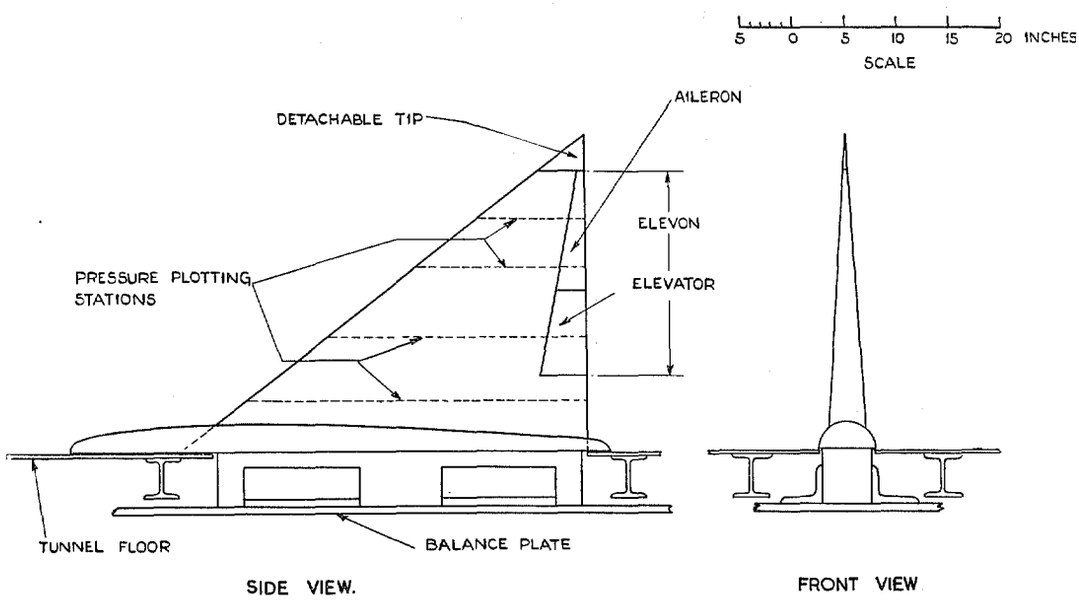


FIG. 1. Installation model in R.A.E. 10-ft × 7-ft High Speed Wind Tunnel.

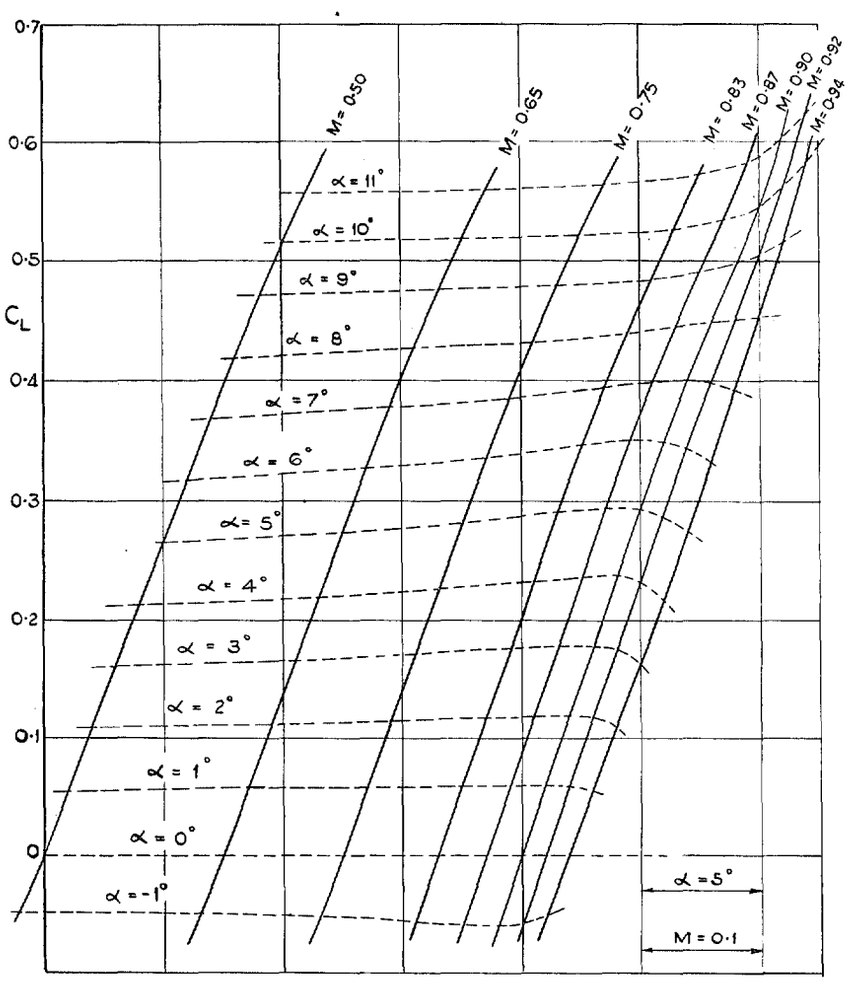


FIG. 2. Lift carpet wing with pointed tip. $R = 1{\cdot}8 \times 10^6$.

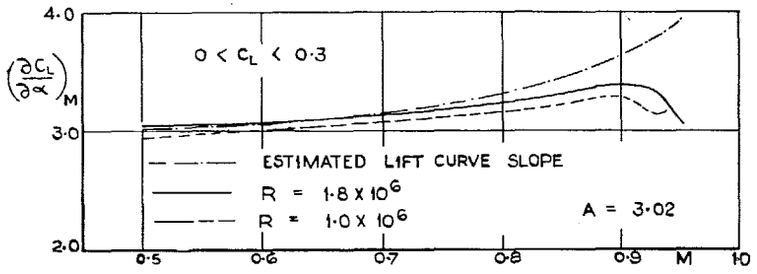


FIG. 3a. Scale effect on lift-curve slope. Model with pointed tip.

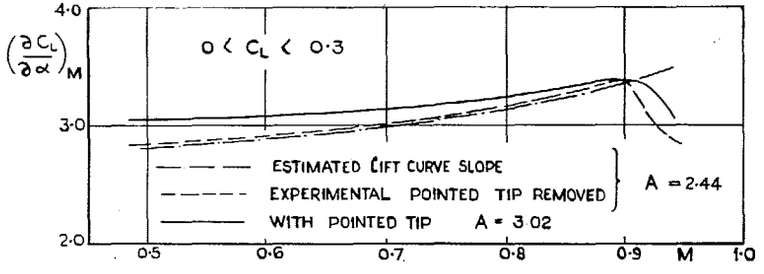


FIG. 3b. Effect of removing pointed tip on lift-curve slope. $R = 1{\cdot}8 \times 10^6$.

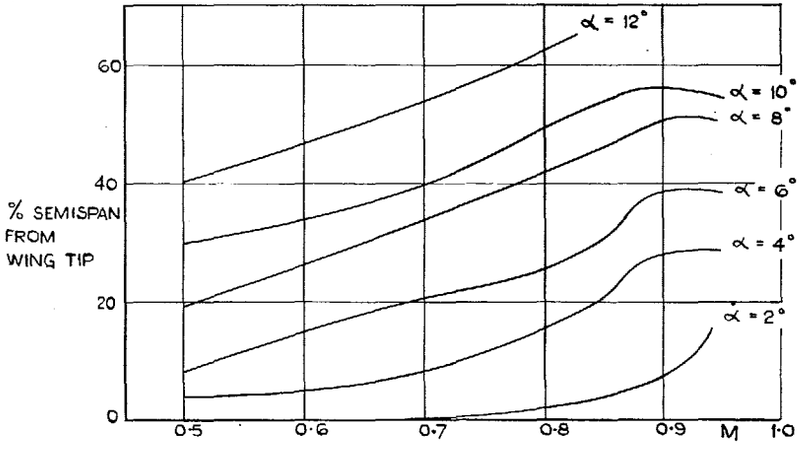


FIG. 3c. Approximate spanwise extent of tip stall for model with pointed tip at $R = 1{\cdot}8 \times 10^6$.

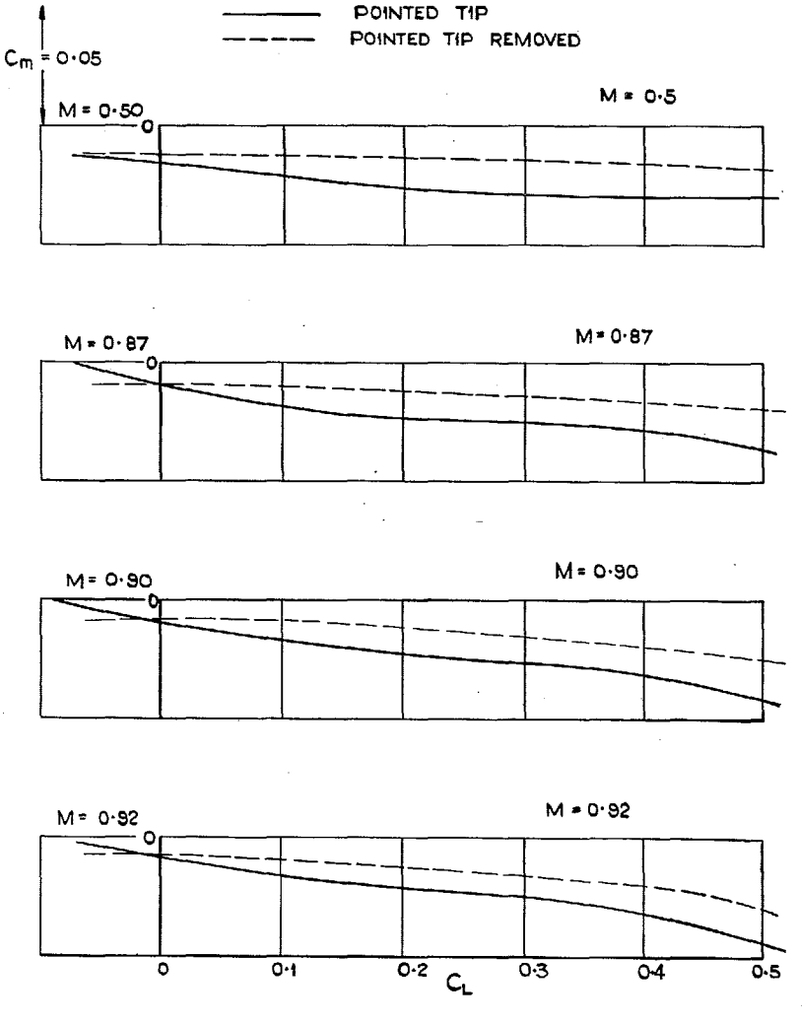


FIG. 4. Effect of removing pointed tip on $C_m$ vs. $C_L$. $R = 1{\cdot}8 \times 10^6$.

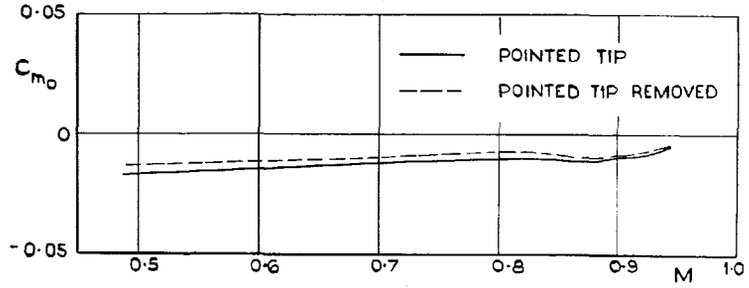


FIG. 5a. Variation of $C_{m0}$ with Mach number.

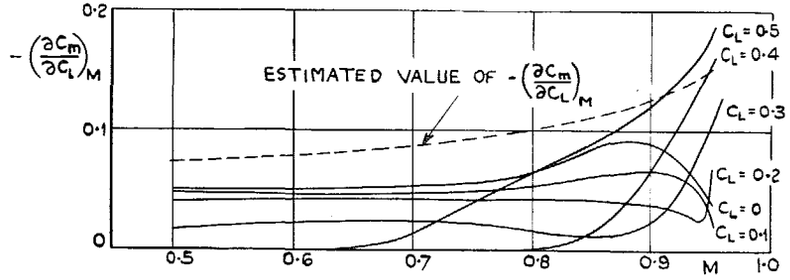


FIG. 5b. Variation of $(\partial C_m/\partial C_L)_M$ with Mach number and $C_L$. Wing with pointed tip.

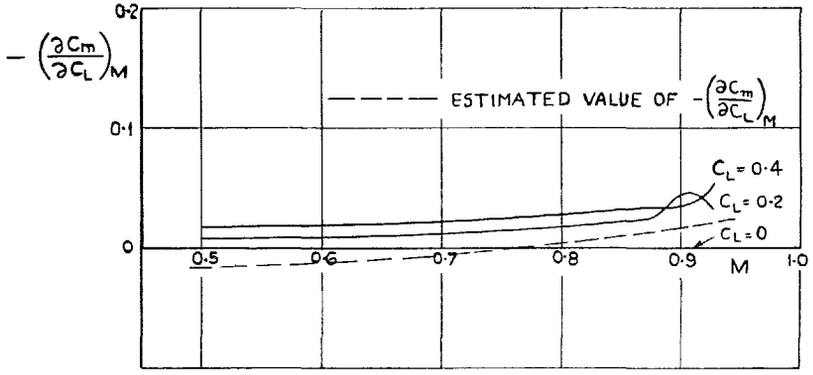


FIG. 5c. Variation of $(\partial C_m/\partial C_L)_M$ with Mach number and $C_L$. Wing with pointed tip removed.

FIGS. 5a, 5b, and 5c. Effect of removing pointed tip on $C_{m0}$ and $(\partial C_m/\partial C_L)_M$. $R = 1·8 \times 10^6$.

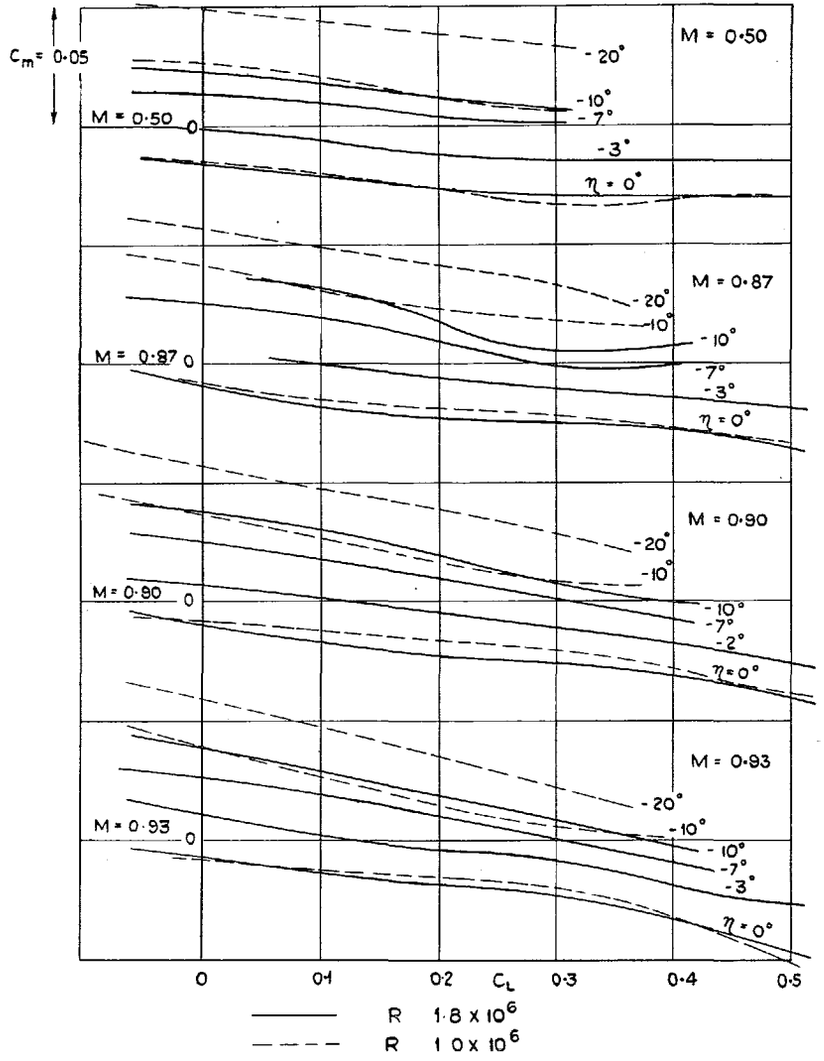


FIG. 6. Effect of elevator on $C_m$ vs. $C_L$.

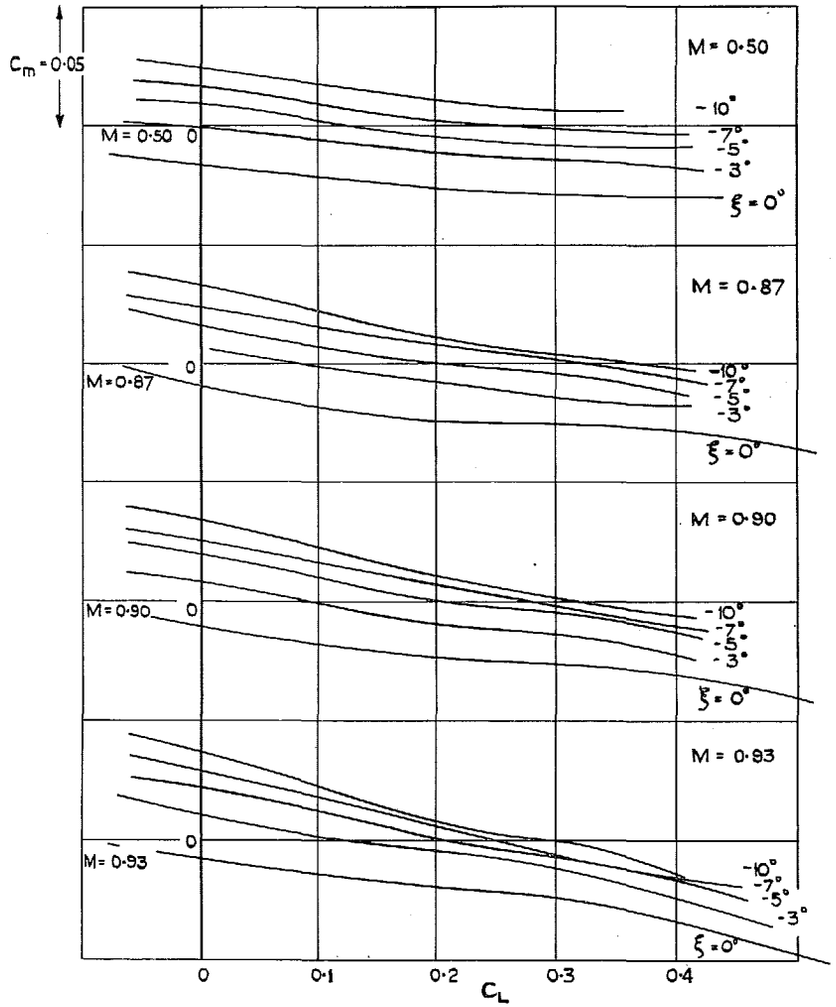


FIG. 7. Effect of aileron on $C_m$ vs. $C_L$. $R = 1{\cdot}8 \times 10^6$.

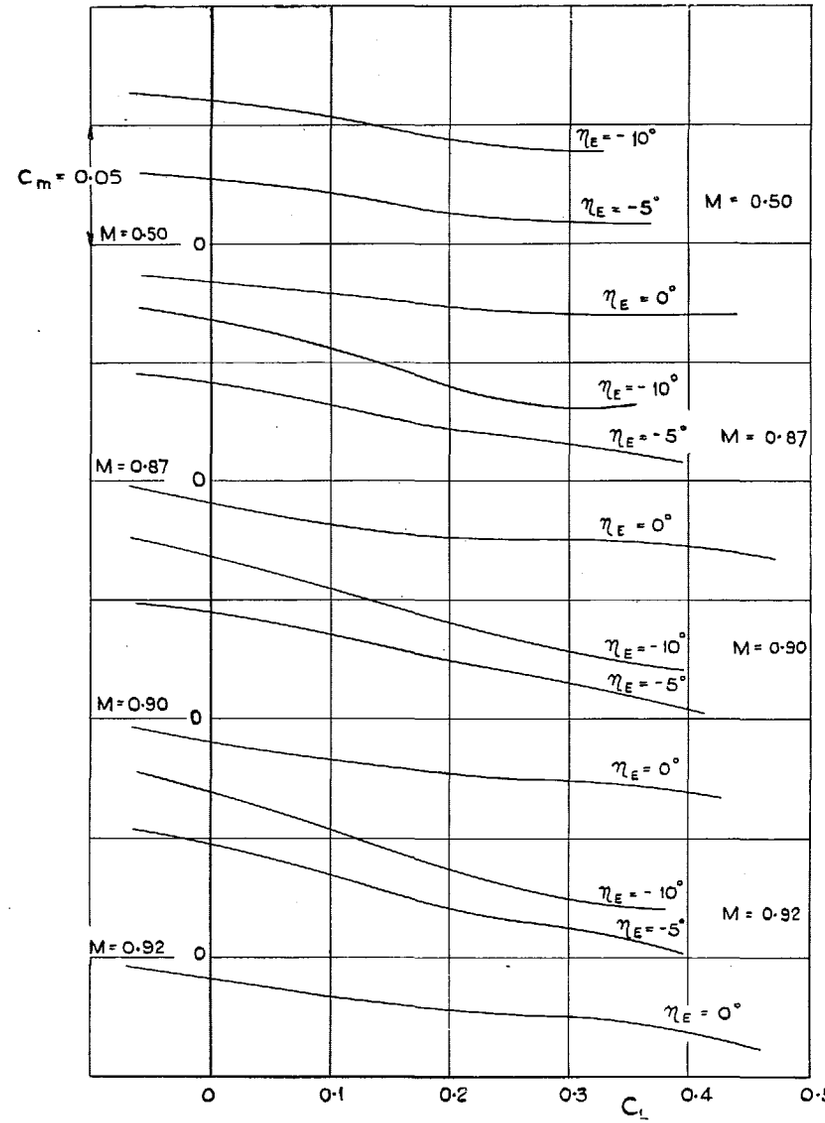


FIG. 8. Effect of elevon on $C_m$ vs. $C_L$. $R = 1{\cdot}8 \times 10^6$.

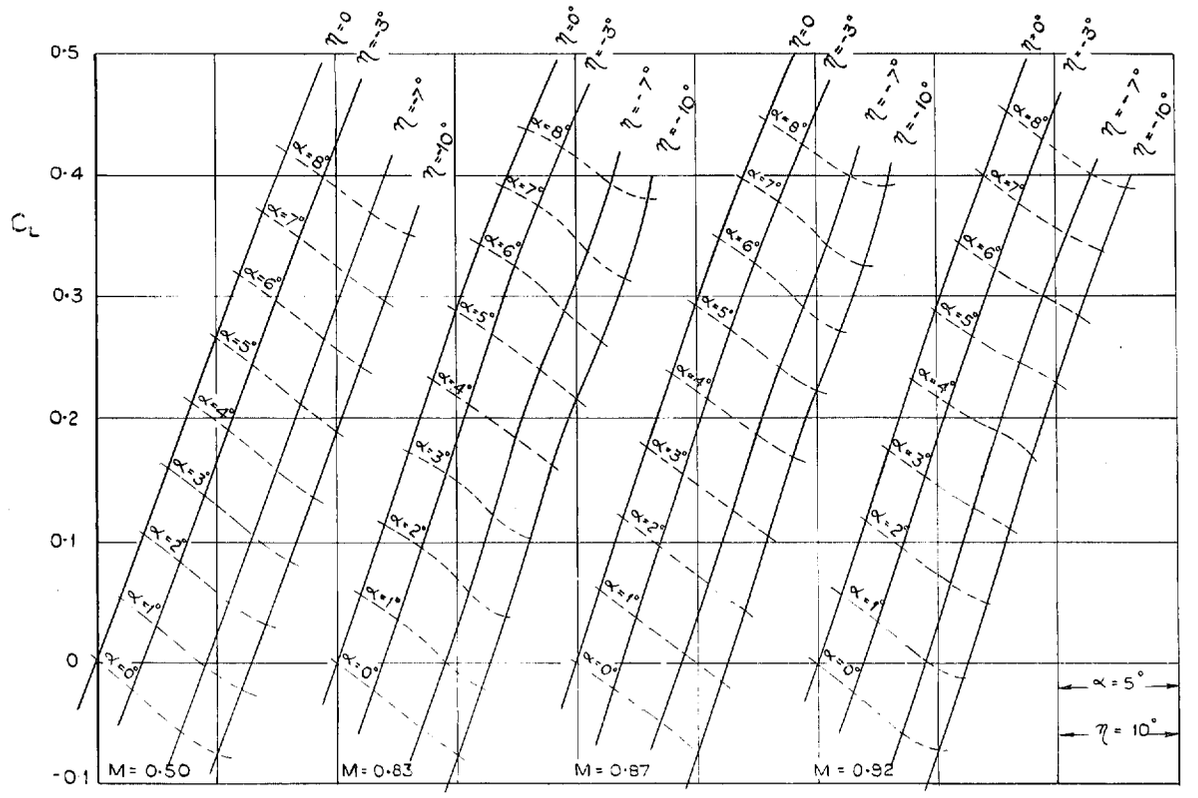


FIG. 9a. Effect of elevator deflection on lift. $R = 1{\cdot}8 \times 10^6$.

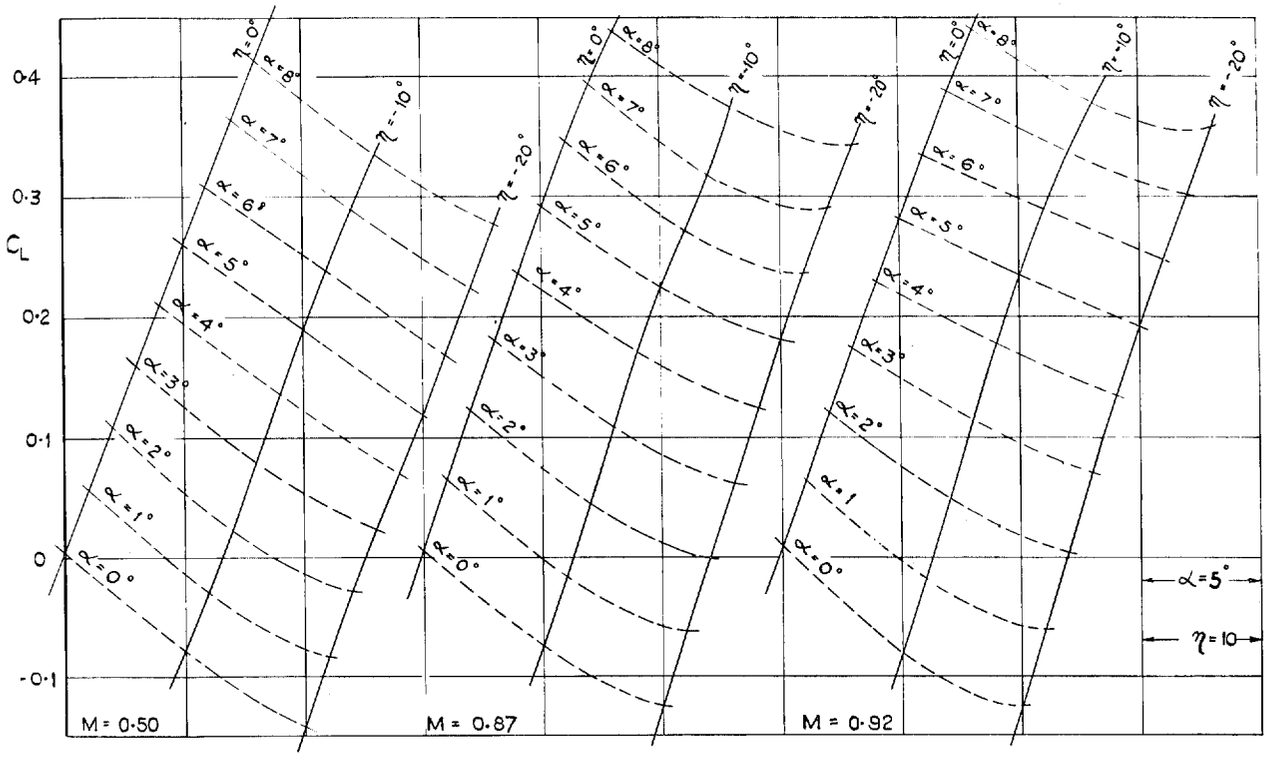


FIG. 9b. Effect of elevator deflection on lift. $R = 1{\cdot}0 \times 10^6$.

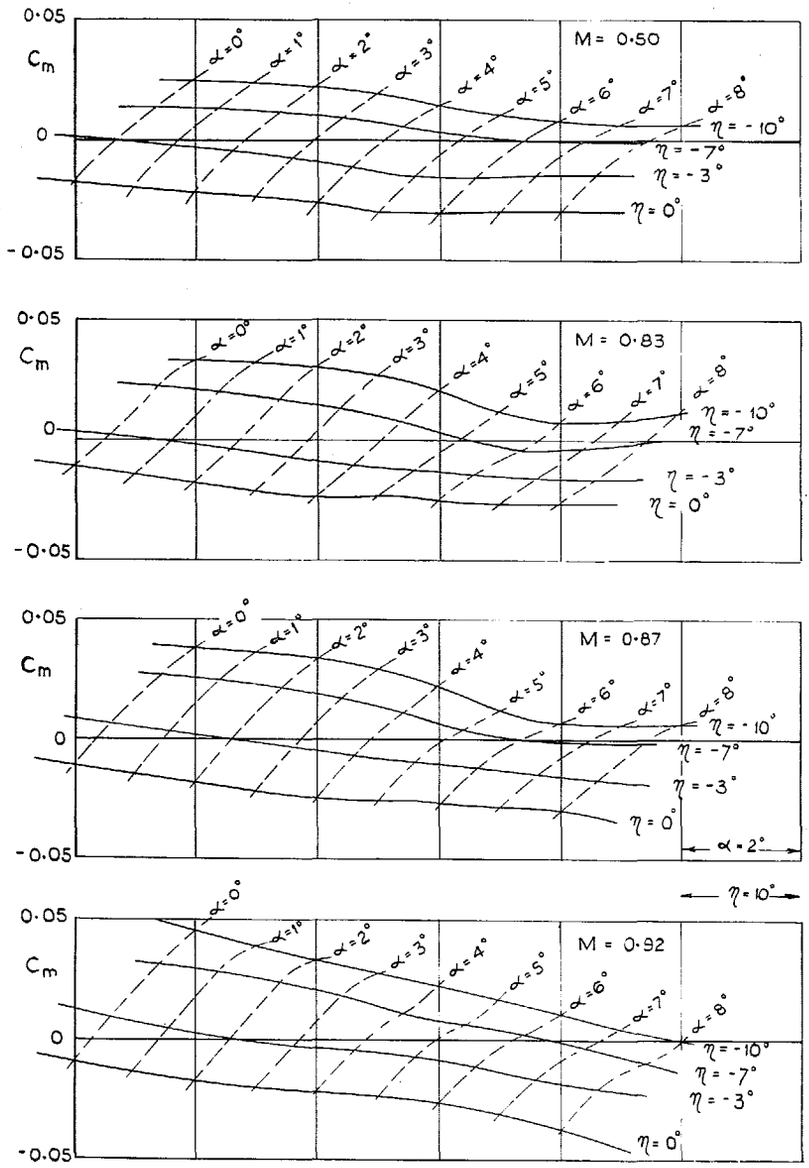


FIG. 10a. Effect of elevator deflection on pitching moment.
$R = 1{\cdot}8 \times 10^6$.

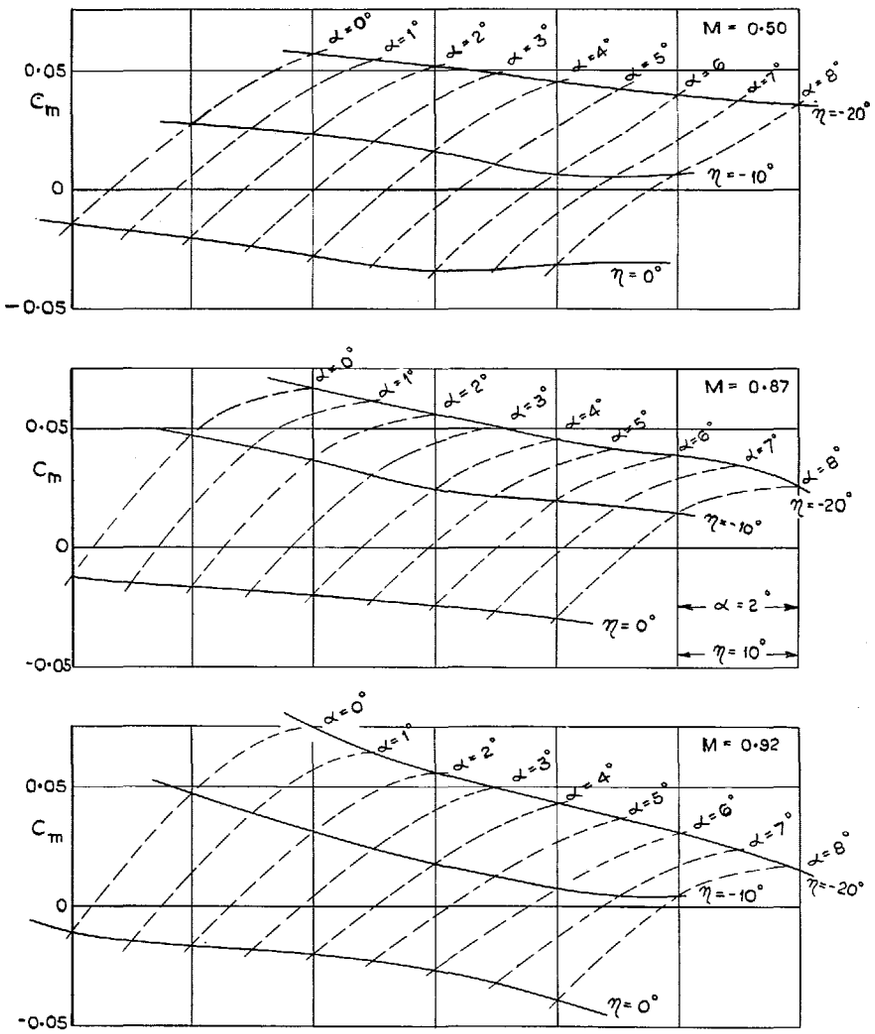


FIG. 10b. Effect of elevator deflection on pitching moment.
$R = 1{\cdot}0 \times 10^6$.

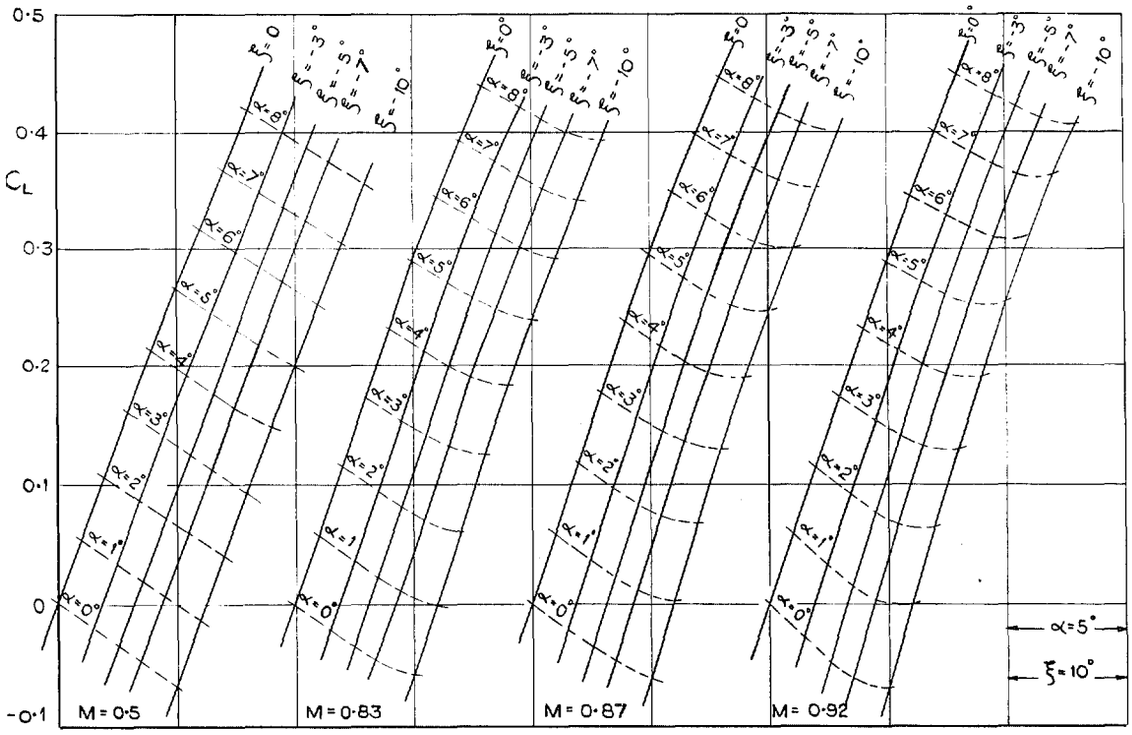


FIG. 11a. Effect of aileron deflection on lift. $R = 1{\cdot}8 \times 10^6$.

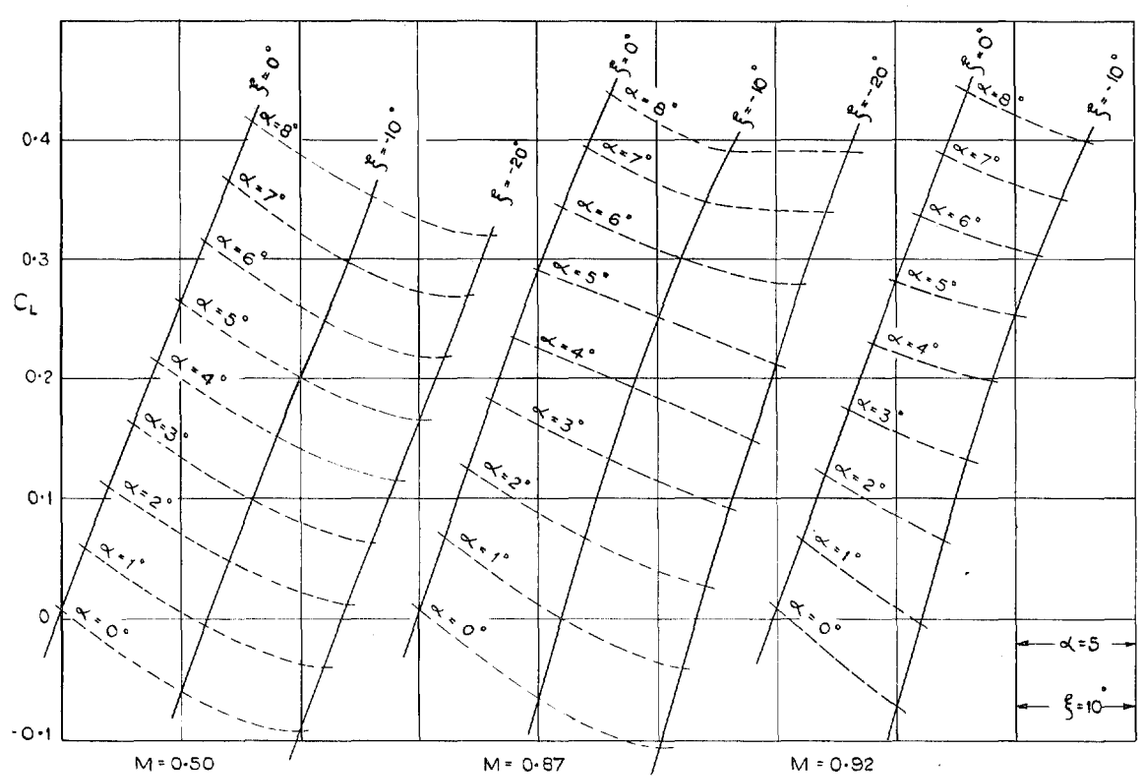


FIG. 11b. Effect of aileron deflection on lift. $R = 1{\cdot}0 \times 10^6$.

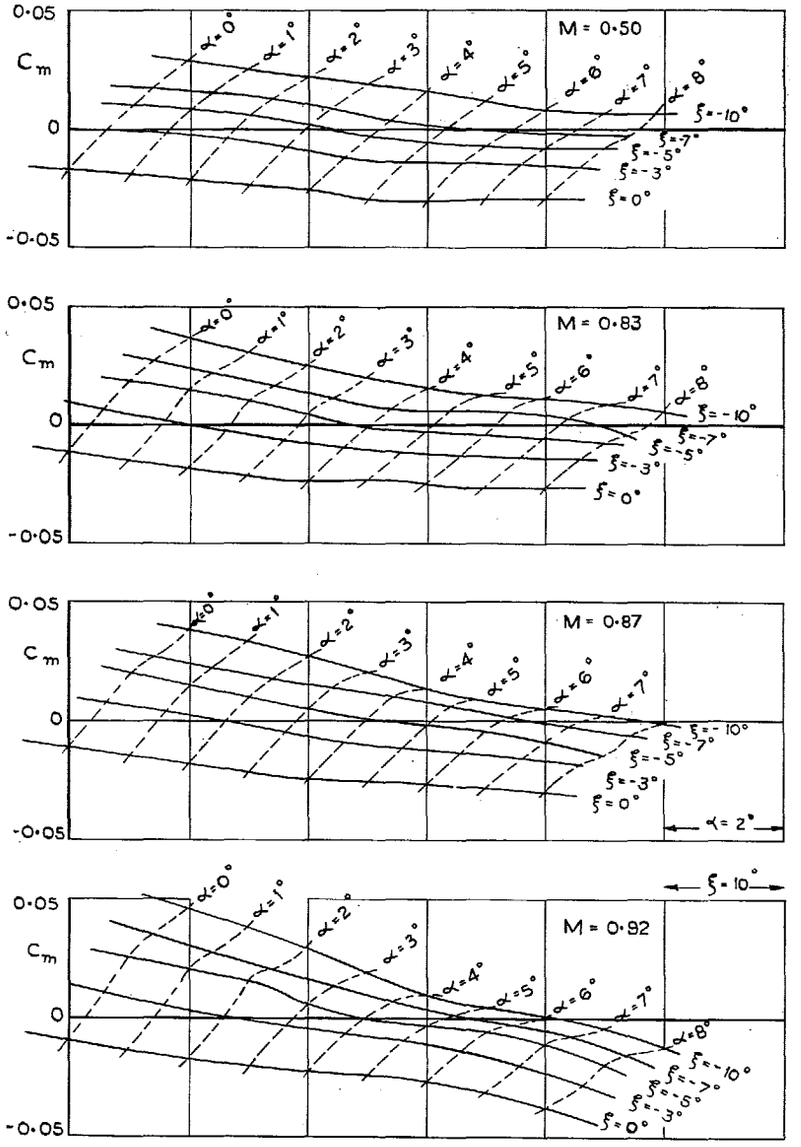


FIG. 12a. Effect of aileron deflection on pitching moment.
$R = 1{\cdot}8 \times 10^6$.

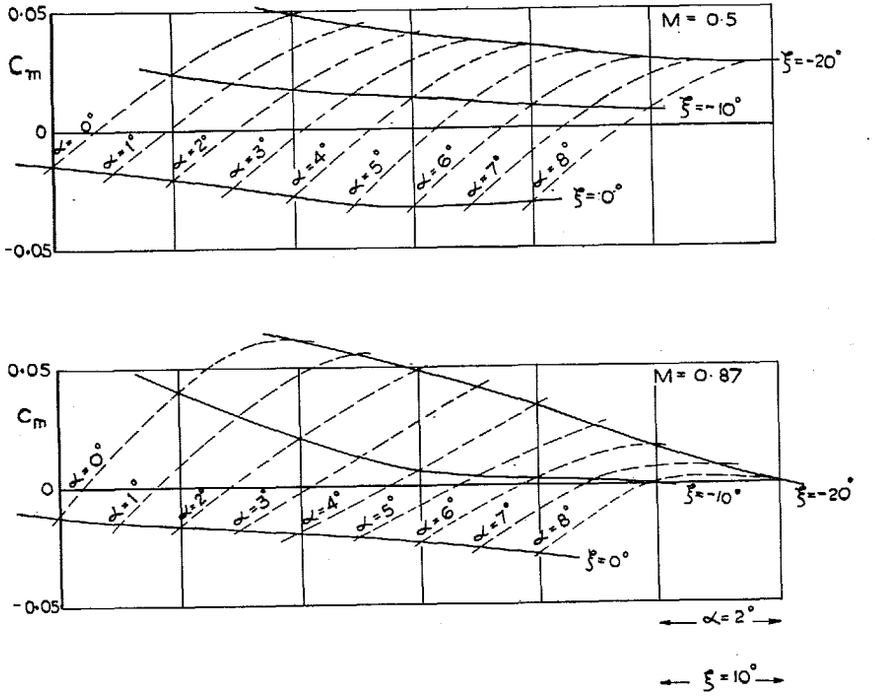


FIG. 12b. Effect of aileron deflection on pitching moment.
$R = 1{\cdot}0 \times 10^6$.

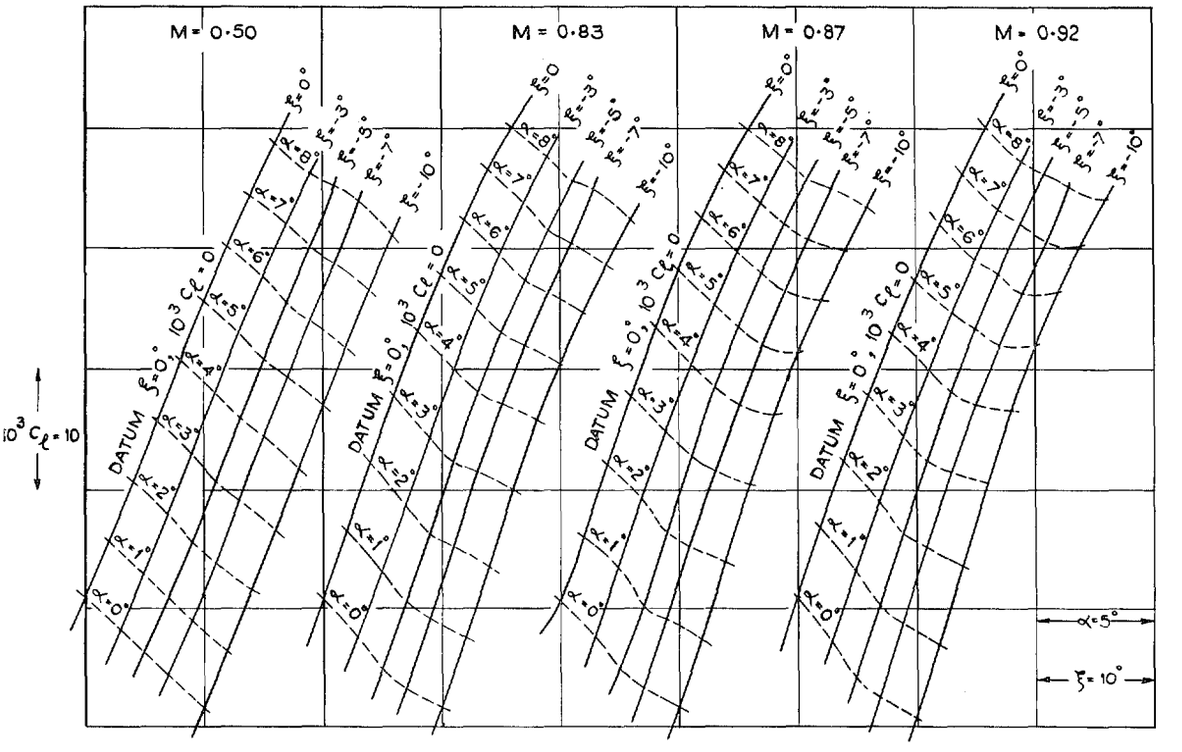


FIG. 13a. Effect of aileron deflection on rolling moment. $R = 1{\cdot}8 \times 10^6$.

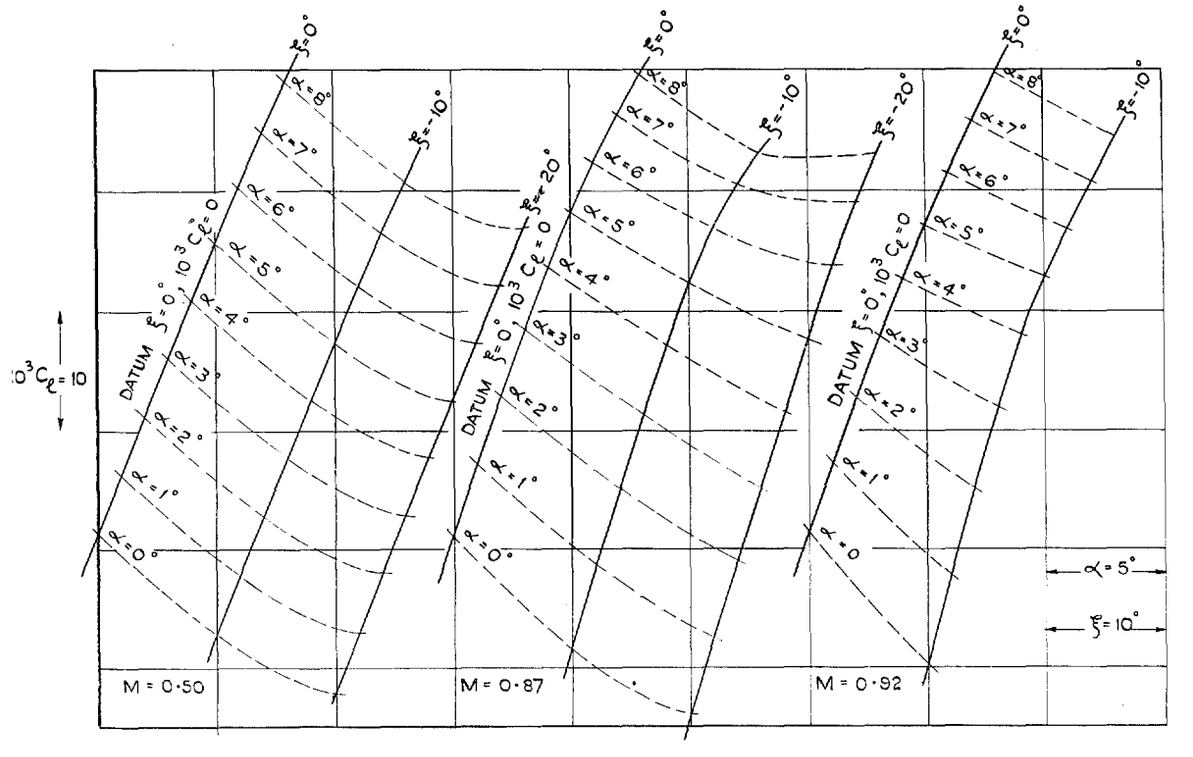


FIG. 13b. Effect of aileron deflection on rolling moment. $R = 1{\cdot}0 \times 10^6$.

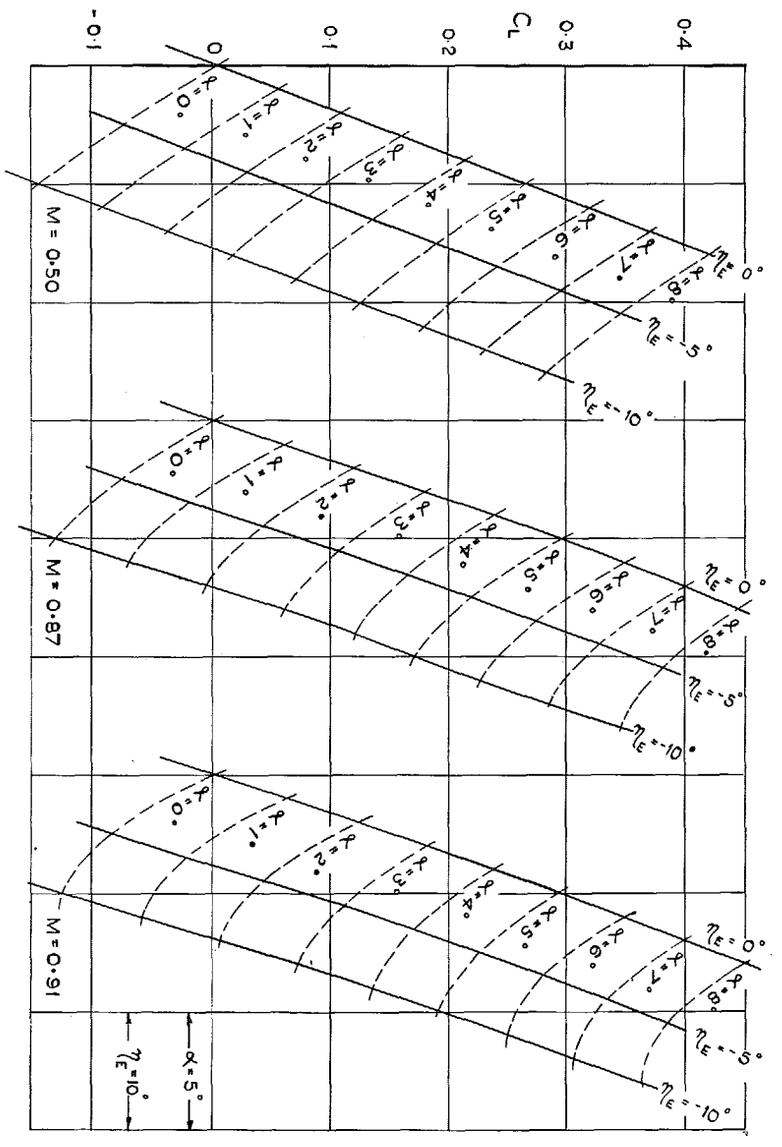


FIG. 14. Effect of elevon deflection on lift. $R = 1{\cdot}8 \times 10^6$.

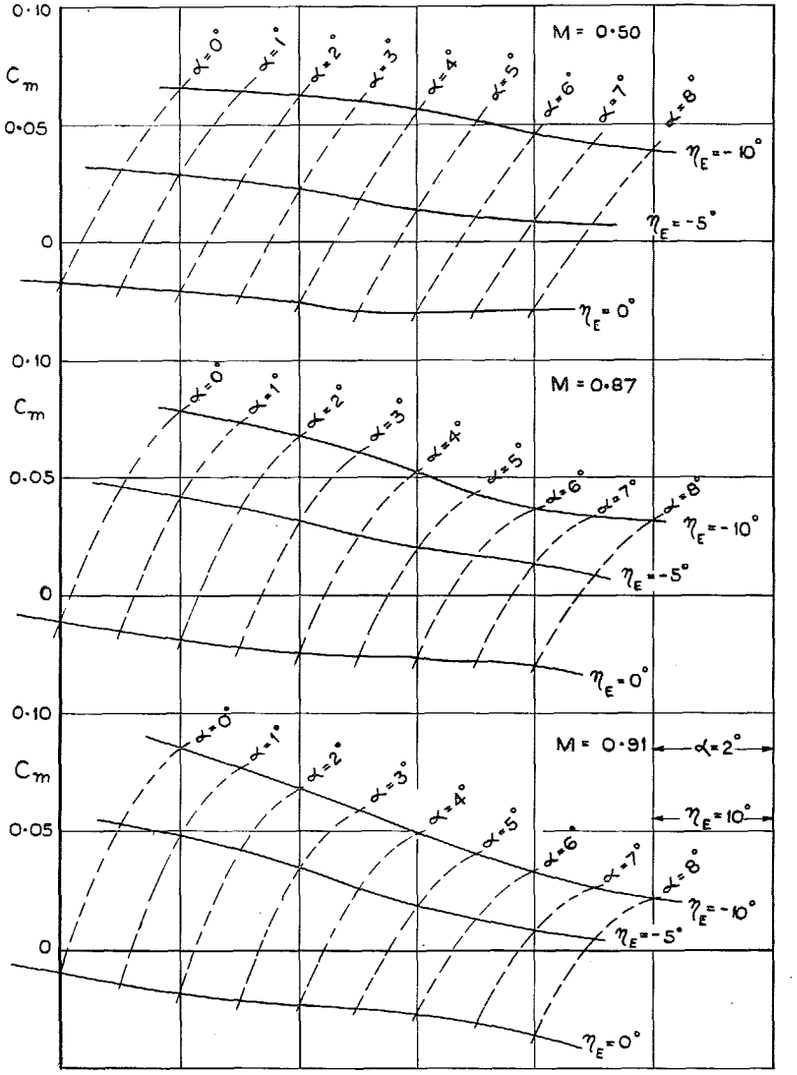


FIG. 15. Effect of elevon deflection on pitching moment. $R = 1{\cdot}8 \times 10^6$.

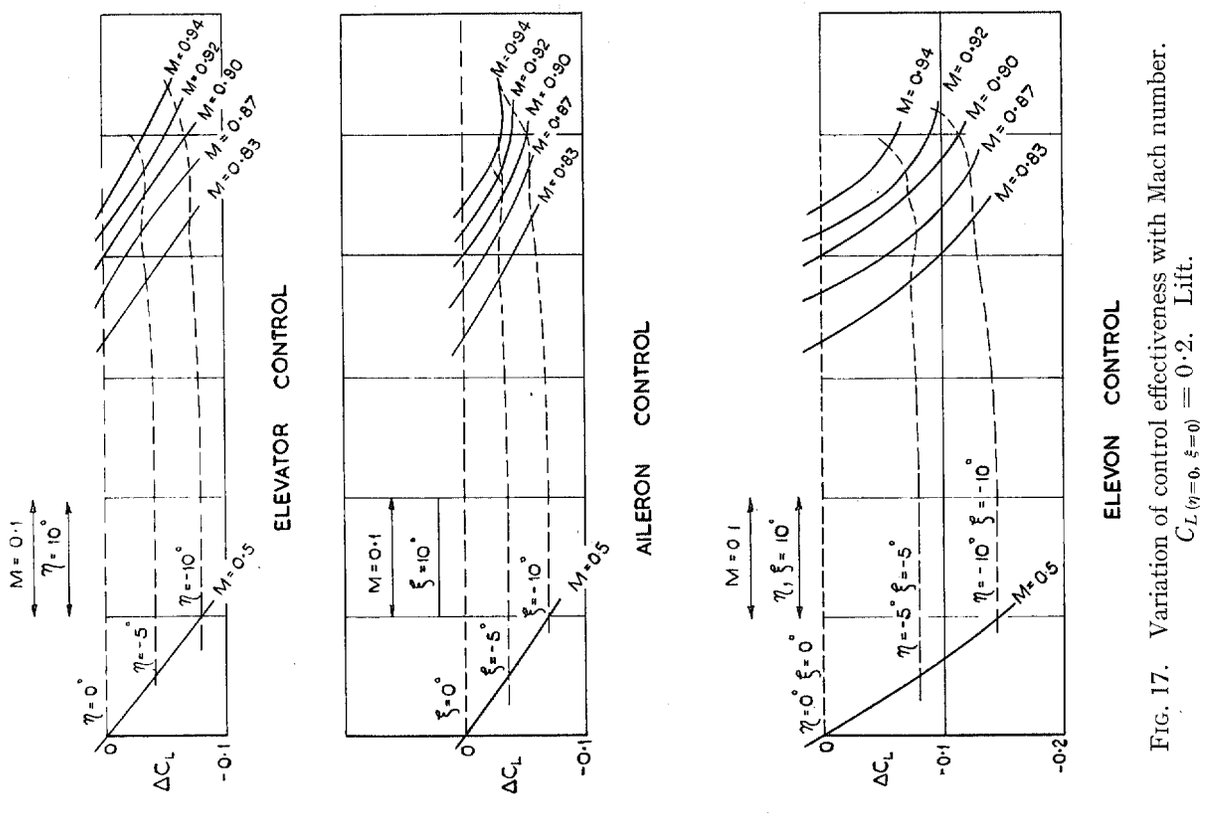


FIG. 17. Variation of control effectiveness with Mach number. $C_{L(\eta=0,\ \xi=0)} = 0{\cdot}2$. Lift.

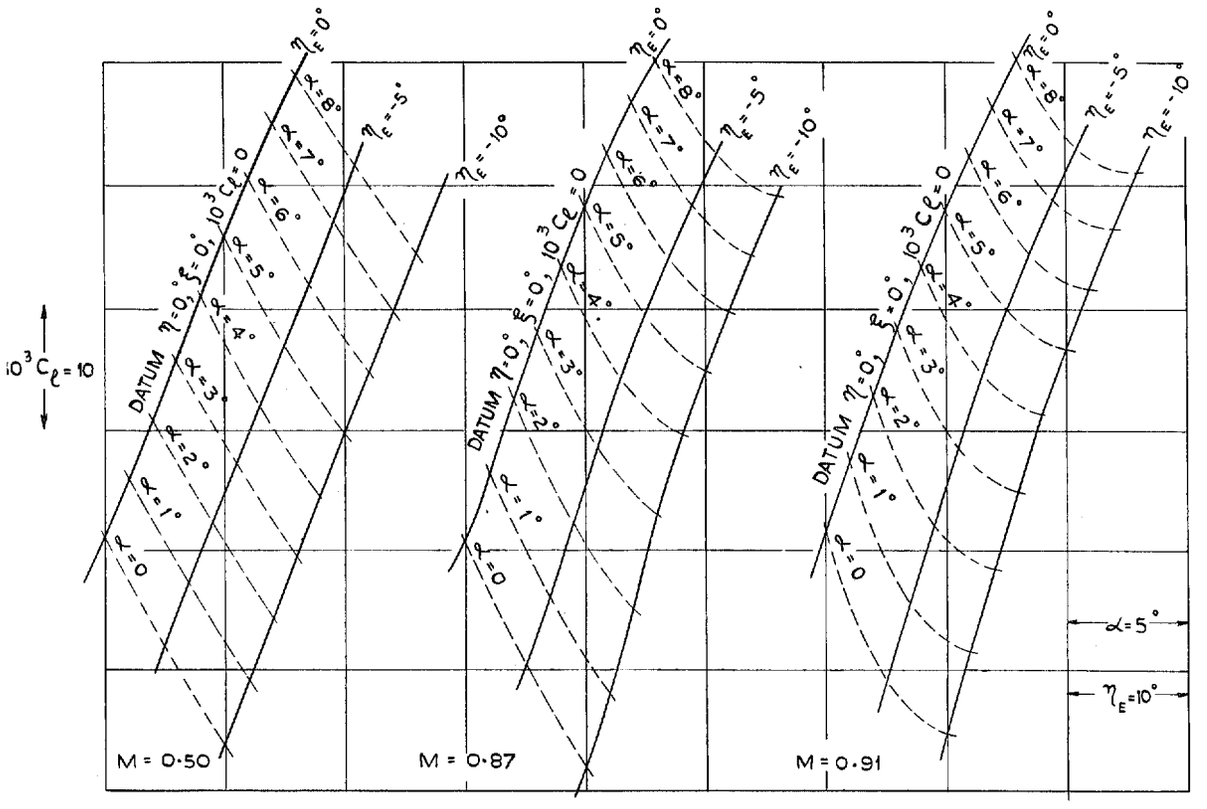


FIG. 16. Effect of elevon deflection on rolling moment. $R = 1{\cdot}8 \times 10^6$.

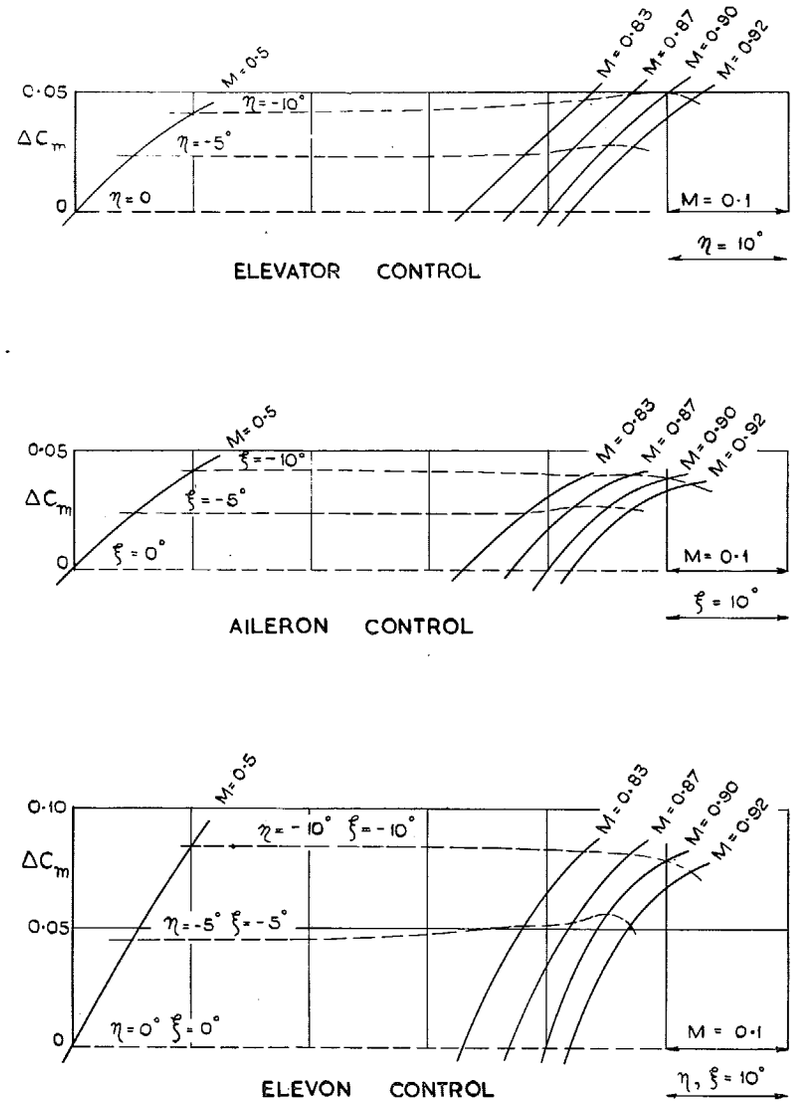


FIG. 18. Variation of control effectiveness with Mach number. $C_{L\,(\eta=0,\ \xi=0)} = 0{\cdot}2$. Pitching moment.

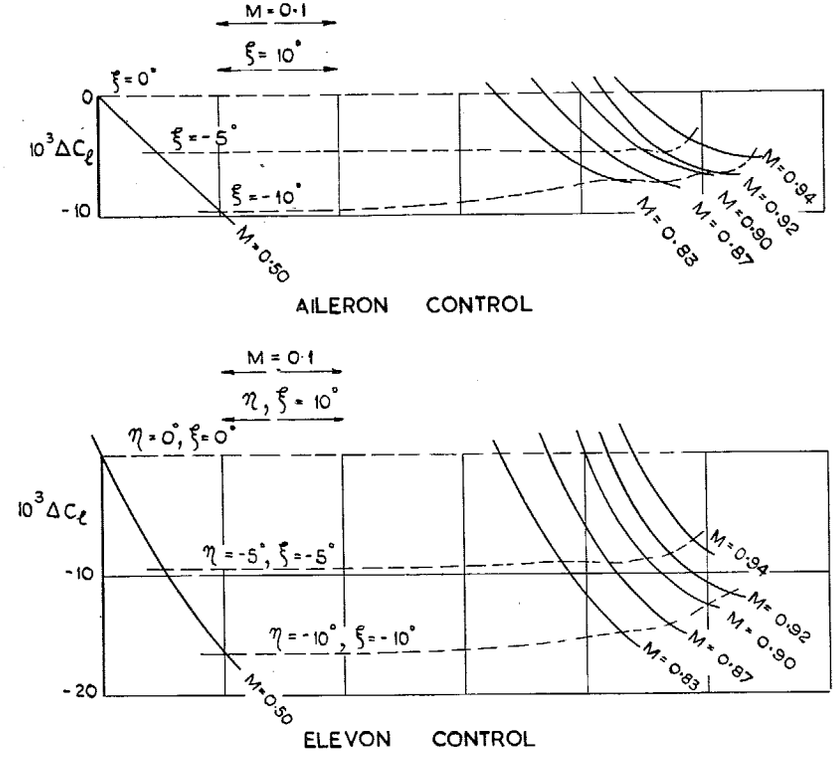


FIG. 19. Variation of control effectiveness with Mach number. $C_{L\,(\eta=0,\ \xi=0)} = 0{\cdot}2$. Rolling moment.

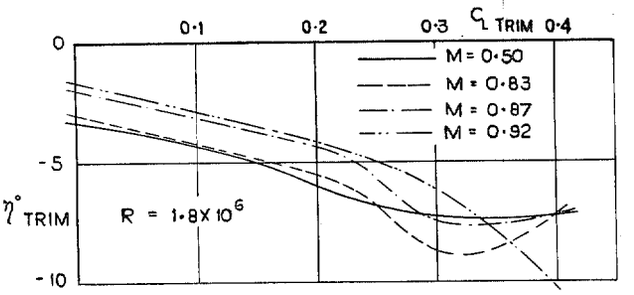


FIG. 20a. Elevator angle to trim.

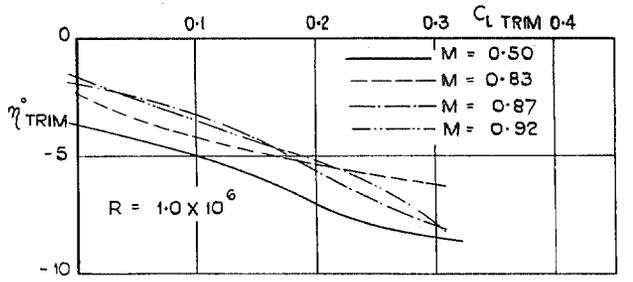


FIG. 20b. Elevator angle to trim.

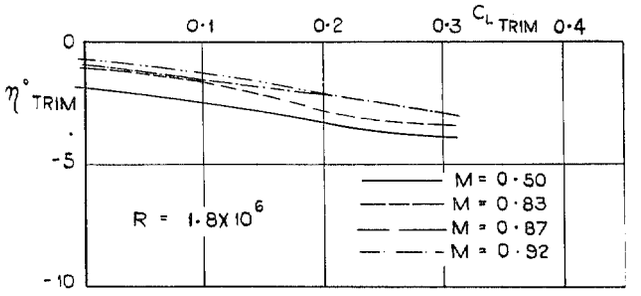


FIG. 20c. Elevon angle to trim.

FIGS. 20a, 20b and 20c. Variation of control angle to trim with Mach number and lift coefficient.



(4967) Wt. 20/9036 K.7 5/57 Hw. PRINTED IN GREAT BRITAIN

# Publications of the Aeronautical Research Council

## ANNUAL TECHNICAL REPORTS OF THE AERONAUTICAL RESEARCH COUNCIL (BOUND VOLUMES)

1939 Vol. I. Aerodynamics General, Performance, Airscrews, Engines. 50*s.* (51*s.* 9*d.*)
Vol. II. Stability and Control, Flutter and Vibration, Instruments, Structures, Seaplanes, etc. 63*s.* (64*s.* 9*d.*)

1940 Aero and Hydrodynamics, Aerofoils, Airscrews, Engines, Flutter, Icing, Stability and Control Structures, and a miscellaneous section. 50*s.* (51*s.* 9*d.*)

1941 Aero and Hydrodynamics, Aerofoils, Airscrews, Engines, Flutter, Stability and Control Structures. 63*s.* (64*s.* 9*d.*)

1942 Vol. I. Aero and Hydrodynamics, Aerofoils, Airscrews, Engines. 75*s.* (76*s.* 9*d.*)
Vol. II. Noise, Parachutes, Stability and Control, Structures, Vibration, Wind Tunnels. 47*s.* 6*d.* (49*s.* 3*d.*)

1943 Vol. I. Aerodynamics, Aerofoils, Airscrews. 80*s.* (81*s.* 9*d.*)
Vol. II. Engines, Flutter, Materials, Parachutes, Performance, Stability and Control, Structures. 90*s.* (92*s.* 6*d.*)

1944 Vol. I. Aero and Hydrodynamics, Aerofoils, Aircraft, Airscrews, Controls. 84*s.* (86*s.* 3*d.*)
Vol. II. Flutter and Vibration, Materials, Miscellaneous, Navigation, Parachutes, Performance, Plates and Panels, Stability, Structures, Test Equipment, Wind Tunnels. 84*s.* (86*s.* 3*d.*)

1945 Vol. I. Aero and Hydrodynamics, Aerofoils. 130*s.* (132*s.* 6*d.*)
Vol. II. Aircraft, Airscrews, Controls. 130*s.* (132*s.* 6*d.*)
Vol. III. Flutter and Vibration, Instruments, Miscellaneous, Parachutes, Plates and Panels, Propulsion. 130*s.* (132*s.* 3*d.*)
Vol. IV. Stability, Structures, Wind Tunnels, Wind Tunnel Technique. 130*s.* (132*s.* 3*d.*)

**Annual Reports of the Aeronautical Research Council—**

1937 2*s.* (2*s.* 2*d.*) 1938 1*s.* 6*d.* (1*s.* 8*d.*) 1939–48 3*s.* (3*s.* 3*d.*)

**Index to all Reports and Memoranda published in the Annual Technical Reports, and separately—**

April, 1950 - - - - R. & M. 2600 2*s.* 6*d.* (2*s.* 8*d.*)

**Author Index to all Reports and Memoranda of the Aeronautical Research Council—**

1909—January, 1954 R. & M. No. 2570 15*s.* (15*s.* 6*d.*)

**Indexes to the Technical Reports of the Aeronautical Research Council—**

| | | |
|---|---|---|
| December 1, 1936—June 30, 1939 | R. & M. No. 1850 | 1*s.* 3*d.* (1*s.* 5*d.*) |
| July 1, 1939—June 30, 1945 | R. & M. No 1950 | 1*s.* (1*s.* 2*d.*) |
| July 1, 1945—June 30, 1946 | R. & M. No. 2050 | 1*s.* (1*s.* 2*d.*) |
| July 1, 1946—December 31, 1946 | R. & M. No. 2150 | 1*s.* 3*d.* (1*s.* 5*d.*) |
| January 1, 1947—June 30, 1947 | R. & M. No. 2250 | 1*s.* 3*d.* (1*s.* 5*d.*) |

**Published Reports and Memoranda of the Aeronautical Research Council—**

| | | |
|---|---|---|
| Between Nos. 2251–2349 | R. & M. No. 2350 | 1*s.* 9*d.* (1*s.* 11*d.*) |
| Between Nos. 2351–2449 | R. & M. No. 2450 | 2*s.* (2*s.* 2*d.*) |
| Between Nos. 2451–2549 | R. & M. No. 2550 | 2*s.* 6*d.* (2*s.* 8*d.*) |
| Between Nos. 2551–2649 | R. & M. No. 2650 | 2*s.* 6*d.* (2*s.* 8*d.*) |

*Prices in brackets include postage*

HER MAJESTY'S STATIONERY OFFICE

York House, Kingsway, London W.C.2; 423 Oxford Street, London W.1 (Post Orders: P.O. Box 569, London S.E.1)
13a Castle Street, Edinburgh 2; 39 King Street, Manchester 2; 2 Edmund Street, Birmingham 3; 109 St. Mary Street, Cardiff; Tower Lane, Bristol, 1; 80 Chichester Street, Belfast, *or through any bookseller.*

S.O. Code No. 23-2999